Journal of Applied Geophysics 195 (2021) 104473

Contents lists available at ScienceDirect

Journal of Applied Geophysics

journal homepage: www.elsevier.com/locate/jappgeo

Estimation of parameters and thickness of a horizontal layer of arbitrary anisotropy from P-wave moveout

Han Xiao [a], Ivan Pšenčík [b,c,*]

[a] College of Geo-Exploration Science and Technology, Jilin University, Changchun, China
[b] Institute of Geophysics, Acad. Sci. of CR, Boční II, 141 31 Praha 4, Czech Republic
[c] Charles University, Faculty of Mathematics and Physics, Department of Geophysics, Ke Karlovu 3, 121 16 Praha 2, Czech Republic

ARTICLE INFO

Keywords:
Traveltime inversion
Reflection moveout
Arbitrary anisotropy
P wave

ABSTRACT

We present an inversion scheme to estimate anisotropy parameters and thickness of a homogeneous layer of arbitrary anisotropy from traveltimes of a reflected P wave. The scheme is based on the weak-anisotropy approximation of P-wave moveout formula. For the description of anisotropy, we use the so-called A-parameters, which represent an alternative to standard elastic moduli specifying anisotropic media, and allow specification of anisotropy of any symmetry, orientation and strength. The proposed scheme allows estimation of, at most, nine of fifteen A-parameters, which describe P-wave propagation in the weak-anisotropy approximation. Therefore, generally, the reconstruction of the P-wave phase-velocity surface from the estimated parameters is impossible. If we deal, however, with higher-symmetry anisotropy (transversely isotropic, orthorhombic) and if information about the orientation of its symmetry elements is available, reconstruction of the phase-velocity surface is possible. Synthetic tests indicate that the inversion scheme works well even in situations, in which the use of other commonly used moveout formulae leads to unsatisfactory results.

1. Introduction

There are various approaches to the parameter estimation from reflection moveout data in media of varying anisotropy. For their overall description, see Tsvankin and Grechka (2011). Our approach is based on the use of the weak-anisotropy approximation and the use of P-wave reflection moveout formulae derived within this approximation, see for example, Pšenčík and Farra (2017) or Farra and Pšenčík (2021).

In the weak-anisotropy approximation, squared reflection traveltime is expanded in terms of weak-anisotropy (WA) parameters instead of the commonly used Taylor expansion of the square of the reflection traveltime in terms of the square of the offset (Tsvankin and Thomsen, 1994; Fomel and Stovas, 2010; Sripanich et al., 2017). Instead of WA parameters, we use here the so-called A-parameters, which were successfully applied in the inversion studies by Pšenčík et al. (2018, 2020). A-parameters (similarly as WA parameters) represent a generalization of parameters introduced by Thomsen (1986) to describe VTI media. In contrast to Thomsen's parameters, A-parameters can be used for the description of anisotropy of arbitrary symmetry, orientation and strength. As shown in Eq. (A.2), they represent linear combinations of stiffness tensor elements. Within the first-order weak-anisotropy approximation, they can be used to describe various seismic quantities and attributes.

Use of the weak-anisotropy approximation has several important advantages. It makes possible to convert "a nonlinear inverse problem that becomes increasingly more complicated for lower medium symmetries" (Grechka et al., 2005) into a linear inverse problem for any symmetry. Moreover, weak-anisotropy approximation allows separation of P- and S-wave propagation. This results in a reduction of the number of sought A-parameters if we concentrate on P waves only. In this article, we concentrate on P waves reflected from the bottom of a single homogeneous layer of arbitrary anisotropy. This seems to be the best start for future generalizations to, for example, multilayered models, converted waves, dipping reflectors, etc. In contrast to Grechka et al. (2005), we try to estimate not only A-parameters specifying the layer, but also its thickness (reflector depth). Inversion for the thickness of the layer is a nonlinear problem, which we solve iteratively.

Our study is in some respect similar to the study of Xiao et al. (2004), who tested various P-wave moveout approximations, but only for a VTI layer. The anisotropy of layers used in this paper may be arbitrary, and we make no a priori assumptions about its symmetry.

As shown by Pšenčík et al. (2018, 2020), in the weak-anisotropy

* Corresponding author at: Institute of Geophysics, Acad. Sci. of CR, Boční II, 141 31 Praha 4, Czech Republic.
E-mail addresses: 1184918974@qq.com (H. Xiao), ip@ig.cas.cz (I. Pšenčík).

https://doi.org/10.1016/j.jappgeo.2021.104473
Received 8 March 2021; Received in revised form 14 August 2021; Accepted 13 October 2021
Available online 20 October 2021

approximation, P waves alone are completely described by fifteen P-wave A-parameters. As shown by Pšenčík and Farra (2017), in the first-order weak-anisotropy approximation, it is impossible to recover all fifteen A-parameters from the P-wave moveout formula. In fact, only nine A-parameters can be recovered. As we show in this paper, even with this reduced number of A-parameters, it is in some cases possible to recover the P-wave phase velocity surface corresponding to the investigated layer.

In the first section, we present an approximate formula for the calculation of traveltimes of a P wave reflected from the bottom of a homogeneous layer of arbitrary anisotropy. Traveltimes are recorded on a horizontal surface of the layer. The formula is modified into two alternative forms, which can be used in the inversion scheme. After a brief description of the inversion scheme in the next section, section with results of several synthetic inversion tests on models of varying anisotropy symmetry and strength follows. The paper ends by a short conclusion section. In Appendix A, the first-order approximation of the P-wave phase-velocity surface for a general anisotropy symmetry is given. The surface is expressed in terms of A-parameters, whose definition is also included in Appendix A. Brief description of the inversion scheme is given in Appendix B, and matrices of the density-normalized elastic moduli used in synthetic tests are given in Appendix C.

2. Theoretical background

2.1. Traveltime formula

We start from equations 13 and 14 of Farra and Pšenčík (2021), which provide an approximate expression for the traveltime T of the P wave reflected from the bottom of a single homogeneous layer of arbitrary anisotropy and orientation, recorded at an arbitrary offset along a horizontal profile of arbitrary azimuth. Farra and Pšenčík (2021) used the so-called weak-anisotropy (WA) parameters. Here, we replace them by A-parameters introduced by Pšenčík et al. (2018), Pšenčík et al. (2020). In the weak-anisotropy approximation, P-wave propagation is specified by fifteen A-parameters defined in Eq. (A.2) of Appendix A.

A-parameters represent a generalization of Thomsen's (1986) parameters introduced for transversely isotropic media with vertical axes of symmetry (VTI media). The set of 21 A-parameters represents an alternative to the set of 21 independent density-normalized elements of the stiffness tensor. They are applicable to anisotropy of any symmetry, orientation and strength. Their use within the weak-anisotropy approximation represents a useful tool for a study of wave propagation in anisotropic media. Properties of A-parameters are very similar to properties of WA parameters, see their detailed description by Farra et al. (2016).

The approximate equation for the traveltime T at an arbitrary offset x along a horizontal profile of an arbitrary azimuth ϕ reads (Farra and Pšenčík, 2021):

$$T^2(x,\phi) = T_0^2 \frac{(1+\bar{x}^2)^3}{P(\bar{x},\phi)}. \tag{1}$$

Here

$$\begin{aligned} P(\bar{x},\phi) \;=\; & (1+\bar{x}^2)^2 + 2\big(\varepsilon_x cos^2\phi + \varepsilon_y sin^2\phi + \eta_z cos^2\phi sin^2\phi \\ & + 2\chi_z cos\phi sin\phi - 2\xi_{16} cos^3\phi sin\phi - 2\xi_{26} cos\phi sin^3\phi\big)\bar{x}^4 \\ & + 2\big(\eta_x sin^2\phi + \eta_y cos^2\phi + \varepsilon_x cos^2\phi + \varepsilon_y sin^2\phi + \varepsilon_z + 2\chi_z sin\phi cos\phi\big)\bar{x}^2 + 2\varepsilon_z. \end{aligned} \tag{2}$$

The symbol $\bar{x}$ in Eq. (1) denotes the normalized offset and T_0 the two-way zero-offset traveltime. They are given by equations:

$$\bar{x} = \frac{x}{2H} \qquad T_0 = \frac{2H}{\alpha}. \tag{3}$$

The symbols ε_x, ε_y, ε_z, η_x, η_y, η_z, χ_z, ξ_{16} and ξ_{26} are nine of fifteen P-wave A-parameters controlling P-wave propagation in the weak-anisotropy approximation. The symbol H denotes the layer thickness (the reflector depth) and α is the reference P-wave velocity of the reference isotropic medium. The values of all A-parameters depend on the choice of the P-wave reference velocity α; Eq. (1) with (2) is, however, *independent* of α.

Eq. (1) with (2) was derived under the weak-anisotropy approximation. Within it, the following assumptions were made. The actual ray of the reflected wave was replaced by a nearby reference ray in an isotropic medium with the reference velocity α. The deviation of the reference ray from the actual ray was considered to be of the first order. The traveltime along it then represents the first-order approximation of the actual traveltime (Fermat principle). Instead of exact ray and phase velocities, their first-order weak-anisotropy approximations (Farra and Pšenčík, 2016) were used. In this approximation, ray and phase velocities are assumed to be equal. Another approximation is the omission of six of fifteen A-parameters whose effect on traveltimes of reflected P wave is of the second order, and the parameters can be neglected. For more details see Pšenčík and Farra (2017).

For the purpose of the inversion, i.e., for the determination of the above nine A-parameters from the observed traveltimes $T_{obs}(x, \phi)$ of P-wave reflected from the bottom of the layer, it is useful to rewrite Eq. (1) with (2) to the form:

$$\begin{aligned} & \varepsilon_x\bar{x}^2(1+\bar{x}^2)cos^2\phi + \varepsilon_y\bar{x}^2(1+\bar{x}^2)sin^2\phi + \varepsilon_z(1+\bar{x}^2) + 2\chi_z\bar{x}^2(1+\bar{x}^2)cos\phi sin\phi \\ & + \eta_x\bar{x}^2 sin^2\phi + \eta_y\bar{x}^2 cos^2\phi + \eta_z\bar{x}^4 cos^2\phi sin^2\phi \\ & - 2\xi_{16}\bar{x}^4 cos^3\phi sin\phi - 2\xi_{26}\bar{x}^4 cos\phi sin^3\phi = \frac{1}{2}(1+\bar{x}^2)^2\big[T_0^2(1+\bar{x}^2)/T_{\rm obs}^2(x,\phi) - 1\big]. \end{aligned} \tag{4}$$

As Eq. (1) with (2), Eq. (4) is also independent of the reference velocity α. We can, therefore, choose any reasonable value of α and consider it known. In this way, Eq. (4) contains ten unknowns: nine A-parameters and the thickness H of the layer. The number of unknown A-parameters can be reduced by one if we realize that for the zero offset, $x = 0$, Eq. (4) yields:

$$\varepsilon_z = \frac{1}{2}\frac{T_0^2 - T_{\rm obs}^2(0)}{T_{\rm obs}^2(0)}. \tag{5}$$

Thus ε_z can be determined independently of the remaining eight A-parameters. In this way, Eq. (4) can be rewritten as:

$$\varepsilon_x\bar{x}^2(1+\bar{x}^2)cos^2\phi+\varepsilon_y\bar{x}^2(1+\bar{x}^2)sin^2\phi+2\chi_z\bar{x}^2(1+\bar{x}^2)cos\phi sin\phi$$
$$+\eta_x\bar{x}^2sin^2\phi+\eta_y\bar{x}^2cos^2\phi+\eta_z\bar{x}^4cos^2\phi sin^2\phi$$
$$-2\xi_{16}\bar{x}^4cos^3\phi sin\phi-2\xi_{26}\bar{x}^4cos\phi sin^3\phi$$
$$=\frac{1}{2}(1+\bar{x}^2)\left[\left(T_0^2(1+\bar{x}^2)/T_{\rm obs}^2(x,\phi)-1\right)\left(1+\bar{x}^2\right)-\left(T_0^2-T_{\rm obs}^2(0)/T_{\rm obs}^2(0)\right)\right]. \quad (6)$$

We can thus choose between two options; to use Eq. (4) for nine unknown A-parameters and H or Eq. (6) for eight unknown A-parameters and H. The parameter ε_z can be determined from Eq. (5). Since the tests with the latter option lead to more satisfactory results, we use the latter option in the following.

If we have a set of N randomly distributed receivers, the ith being specified by the azimuth ϕ_i and the offset x_i, Eqs. (6) and (5) can be applied at any of them. Resulting system of equations can be used for the estimate of the nine P-wave A-parameters. If the thickness H of the layer is not known, it can be estimated by using the following procedure. First, an interval, in which the sought H is expected, must be specified. Then, for each of the selected values of H from the chosen interval, the eight A-parameters ε_x, ε_y, η_x, η_y, η_z, ξ_{16}, ξ_{26} and χ_z are determined by solving Eq. (6) and ε_z is obtained from Eq. (5). In the following step, estimated A-parameters are inserted to Eq. (1) with (2) to obtain the approximate traveltime $T(x_i, \phi_i)$ for all of N receivers. From all tested values of H, we seek the one, which minimizes the average T_{AV} of relative traveltime errors from all N receivers:

$$T_{\rm AV}=N^{-1}\sum_{i=1}^{N}|T(x_i,\phi_i)-T_{\rm obs}(x_i,\phi_i)|/T_{\rm obs}(x_i,\phi_i)\times 100\%. \quad (7)$$

It is important to emphasize one aspect of the above-described procedure. As shown by Pšenčík and Gajewski (1998), the first-order P-wave phase velocity used in the derivation of Eq. (1) with (2) is always less than or equal to the exact phase velocity. This means that the inversion for the true H yields A-parameters leading to higher phase velocity and, as a consequence, shorter traveltimes. Since ε_z determined from Eq. (5) guarantees zero-offset traveltime $T(0)=T_{obs}(0)$, the approximate traveltimes for non-zero offsets will be shorter than exact ones. This seems to indicate reflections from a deeper reflector. In other words, due to its approximate basis, the described procedure tends to overestimate the values of the layer thickness H. Numerical tests reveal that this overestimation amounts, at most, to 5% of the value of H. Only in extreme cases, as shown in the following, it may reach 10%.

2.2. Inversion scheme

For N source-receiver pairs, it is possible to arrange Eq. (6) to the form of a system of N linear equations for the determination of eight unknown P-wave A-parameters from N observed reflected P-wave traveltimes $T_{obs}(x_i, \phi_i)$ recorded at N randomly distributed receivers. In the matrix form we can write:

$$\mathrm{Gm}=\mathrm{d}. \quad (8)$$

Here **G** represents an $N \times M$ matrix, where N is the number of receivers and M is the number of sought A-parameters, in our case $M = 8$. The rows of matrix **G** have the form shown in Eq. (B.2). Each row in matrix **G** corresponds to one particular receiver. Symbol **m** in Eq. (8) denotes the vector of model parameters to be determined. In our case, it consists of eight P-wave A-parameters, see Eq. (B.3) (ε_z is determined independently from Eq. (5)). Vector **d** in Eq. (8) contains known quantities, specifically observed traveltimes $T_{obs}(x_i, \phi_i)$, normalized offsets $\bar{x}_i$, azimuths ϕ_i, and the zero-offset traveltime T_0. The explicit form of the vector **d** is given in Eq. (B.4).

Eq. (8) is solved by means of pseudoinverse described in Appendix B, see Eqs. (B.5)–(B.8).

3. Inversion tests

Program package ANRAY (Gajewski and Pšenčík, 1990) was used to generate traveltimes of P-waves reflected from the bottoms of homogeneous layers of several anisotropy symmetries. These traveltimes were considered as observed traveltimes $T_{obs}(x_i, \phi_i)$. They were generated by the source situated at the center of an 8×8 km region, and recorded by 51 receivers, specified by offsets x_i and azimuths ϕ_i, irregularly distributed in the region, see the top plot in Fig. 1. The bottom plot shows the sketch of the model with definitions of the offset and thickness of the layer. One of the receivers is situated exactly in the center of the 8×8 km region, and thus allowed direct measurement of the zero-offset traveltime $T_{obs}(0)$. Anisotropy of varying type of symmetry, strength and orientation was considered. Here we consider two types of anisotropy: transverse isotropy with vertical axis of symmetry (VTI) and triclinic symmetry (TRI). Tests with other types of anisotropy, as transverse isotropy with tilted axis of symmetry (TTI) or tilted orthorhombic symmetry (TOR) can be found in Xiao and Pšenčík (2020). The anisotropy strength is defined as $2(c_{max}-c_{min})/(c_{max}+c_{min}) \times 100\%$, where c_{max} and c_{min} denote maximum and minimum phase velocities. The reference velocity α of the reference isotropic medium used for the definition of A-parameters, see Eq. (A.2), and for the reference two-way zero-offset traveltime T_0, see Eq. (3), is chosen as $\alpha = 3.6$ km/s in all tests. Traveltimes generated by the package ANRAY with either no noise or with added random Gaussian noise of 2 ms and 4 ms are inverted. In contrast to Pšenčík et al. (2020), in which real noise extracted from the field data was used, we use random Gaussian noise. It allows us to estimate the robustness of the proposed approach with respect to distortions in data.

Tests with traveltimes of the P-wave reflected from the bottom of a homogeneous isotropic layer lead to effective equality of A-parameters ε_x, ε_y and ε_z, with remaining six A-parameters being zero. This was an indication that the layer was isotropic, see Eq. (A.4). When noisy

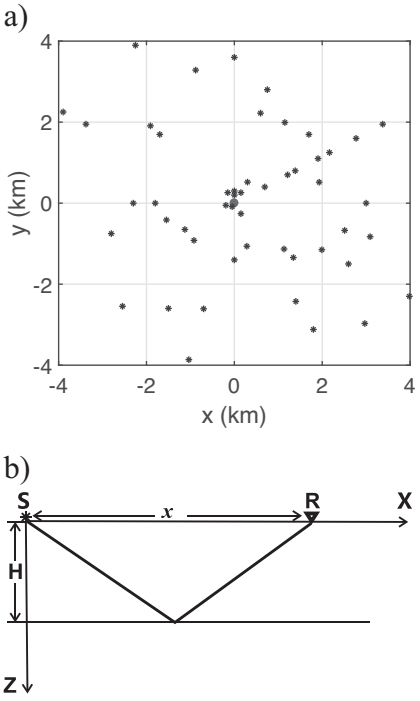

Fig. 1. Top: distribution of 50 irregularly distributed surface receivers (stars) around the source (full circle; $x = y = 0$ km; the source coincides with the receiver situated at the origin of coordinates), at which reflection traveltimes used for the inversion are generated. Bottom: sketch of the model; offset x between the source S and the receiver R, H – the layer thickness (the reflector depth).

traveltimes were inverted, the resulting A-parameters were estimated with small errors. The thickness H was slightly overestimated, always by less than 5%.

Tests with anisotropic layers lead to estimates of A-parameters with greater errors, and greater overestimates of the thickness H of the layer, usually not exceeding 5%. Only in extreme cases as the model B below, the overestimate reached nearly 10%. The errors of the estimates of A-parameters increased with increased strength of anisotropy. The overestimates of H increased mostly with increase of H. For the illustration of the performance of the proposed inversion scheme, we show, in the following, results of inversion for three models.

In the first model, model A, we invert traveltimes of the wave reflected from the bottom of a weakly anisotropic VTI layer whose anisotropy strength is approximately 8%. The thickness of the layer is $H = 0.2$ km. The 6×6 matrix of the density normalized elastic moduli in the crystal coordinate system in Voigt notation is shown in Eq. (C.1). A-parameters of the VTI layer, see Eq. (A.3), are $\varepsilon_x = -0.1$, $\varepsilon_z = -0.153$ and $\eta_y = 0.04$.

The first step is the search for the thickness H of the layer. This procedure is illustrated in Fig. 2, which shows the plots of relative traveltime differences $(T_H - T_{obs})/T_{obs}$ as a function of the offset. Traveltime T_H is calculated from Eq. (1) with (2), in which the assumed thickness H and A-parameters inverted for this thickness H are used. In Fig. 2a noiseless traveltimes, in Fig. 2b and c traveltimes with 2 ms and 4 ms Gaussian random noise, respectively, are used. Five thicknesses are tested, $H = 0.1$, 0.2, 0.3, 0.4 and 0.5 km. Traveltime errors corresponding to different values of H are denoted by different symbols. Bold symbols are used for such a value of H, for which T_{AV} in Eq. (7) is minimum. Because the true H is small, $H = 0.2$ km, the overestimate of H is negligible, and T_{AV} is minimum for $H = 0.2$ km for noiseless as well as noisy data. For greater values of H, its overestimation may occur, see Xiao and Pšenčík (2020).

Variation of estimated A-parameters with assumed layer thickness H for traveltimes with 4 ms random noise is shown in Fig. 3. In it, we can see several interesting phenomena. We can see that the only A-parameters significantly varying with H are ε_z, η_x and η_y. The rest of A-parameters remains effectively independent of H, with their values close to zero. This result is not surprising after the inspection of Eq. (A.1) for the P-wave phase velocity. It shows that the vertical and nearly vertical propagation is prevailingly affected by the A-parameters ε_z, η_x and η_y. Without estimating the thickness H of the layer, Fig. 3 allows to guess that the layer is VTI. A-parameters η_z, ε_{16}, ε_{26} and χ_z are effectively zero for any value of H, and for nearly all values of H, $\varepsilon_x = \varepsilon_y$ and $\eta_x = \eta_y$. According to Eq. (A.3), such a specification corresponds to the VTI

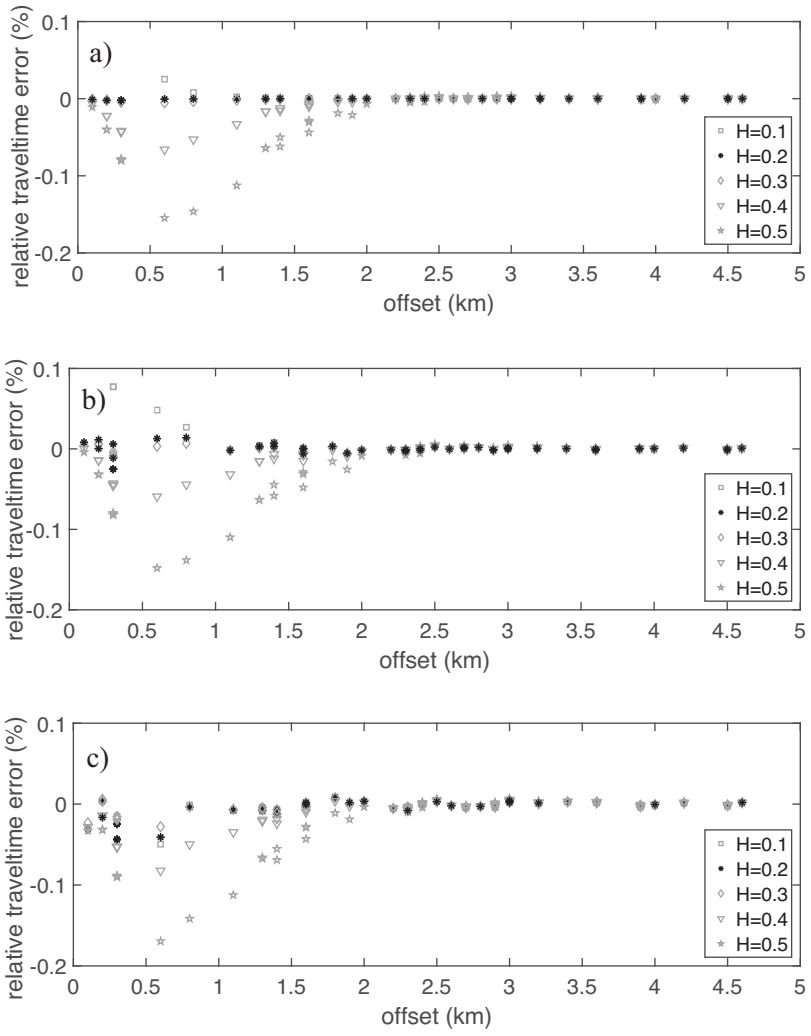

Fig. 2. Relative traveltime errors $(T - T_{obs})/T_{obs}$ versus offset for the model A (VTI) for thickness H varying from 0.1 to 0.5 km. (a) No noise, (b) 2 ms and (c) 4 ms random Gaussian noise added to traveltimes generated by ANRAY package. Bold symbols correspond to thicknesses with minimum average T_{AV} of relative traveltime errors, see Eq. (7).

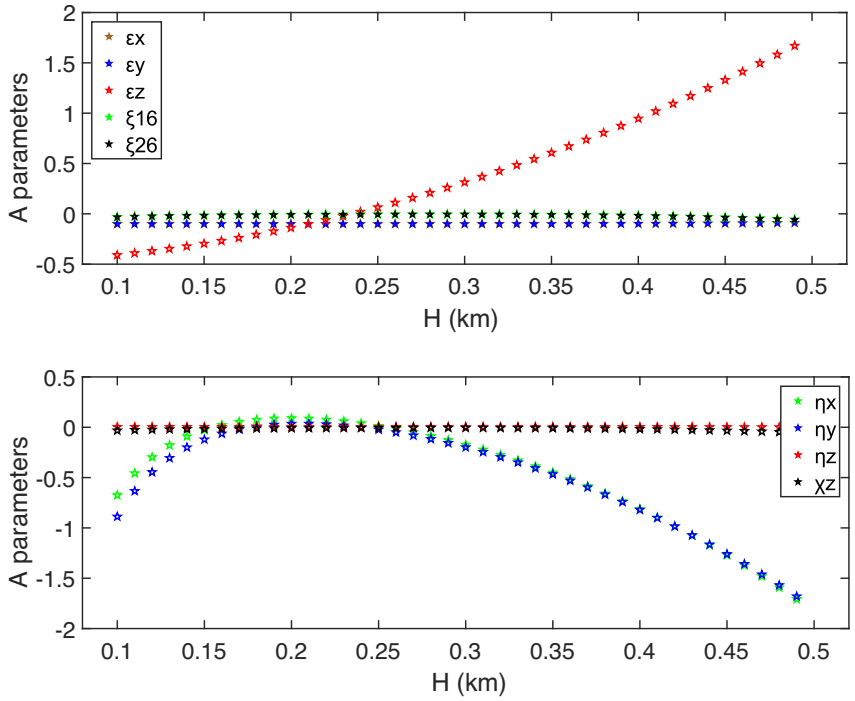

Fig. 3. Variation of estimated A-parameters with assumed thickness H in the model A (VTI). Reference velocity $\alpha = 3.6$ km/s, traveltimes with 4 ms random Gaussian noise used.

symmetry.

Model covariance matrix related to the inversion of traveltimes with 4 ms random Gaussian noise generated in the model A, shown in Fig. 4, slightly differs from the matrix obtained by Pšenčík et al. (2020). First of all, the matrix in Fig. 4 shows only 8 A-parameters (ninth parameter ε_z is determined separately from Eq. (5)). Next, the parameters with greatest variation are η_x and η_y. These two parameters are also most strongly correlated. The variations and correlations of parameters χ_z, ξ_{16} and ξ_{26} are similar to the study of Pšenčík et al. (2020). The remaining A-parameters, ε_x, ε_y and η_z have only weak variations and correlations. There are two phenomena, which affect the described character of the covariance matrix: anisotropy symmetry and the noise level. Intensity of variations and correlations of A-parameters increases with increasing number of non-zero A parameters. Intensity of variations and correlations for the same noise level depends on the thickness H of the layer. For small H the effects are more pronounced because traveltimes are smaller, and thus more affected by the noise.

Results of the inversion of noiseless and noisy data for optimum values of H minimizing T_{AV} in Eq. (7) are shown in Fig. 5, in which estimated (circles) A-parameters are compared with true (squares) A-parameters. The thick vertical lines are the error bars introduced in Appendix B. The error bars are three times increased for better visibility. Fig. 5a shows results of the inversion of the noiseless traveltimes, Fig. 5b and c show results with random Gaussian noise of 2 ms and 4 ms, respectively. Due to weak anisotropy of the layer, we can see the perfect fit of A-parameters estimated from noise-free data with true parameters

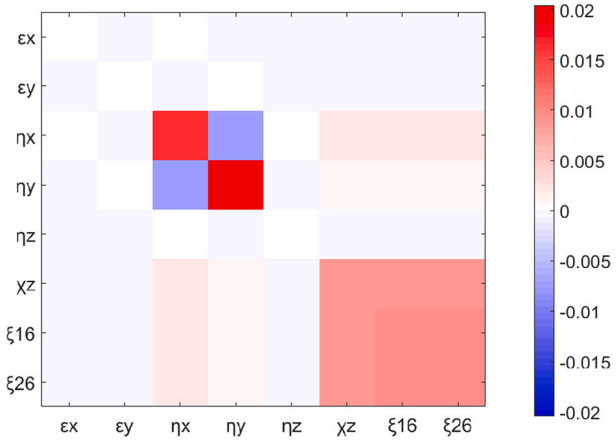

Fig. 4. Model covariance matrix related to the inversion of traveltimes in the model A (VTI) with 4 ms random Gaussian noise added to traveltimes generated by ANRAY package. Diagonal elements indicate the variation of A-parameters. The off-diagonal elements indicate the correlation between A-parameters.

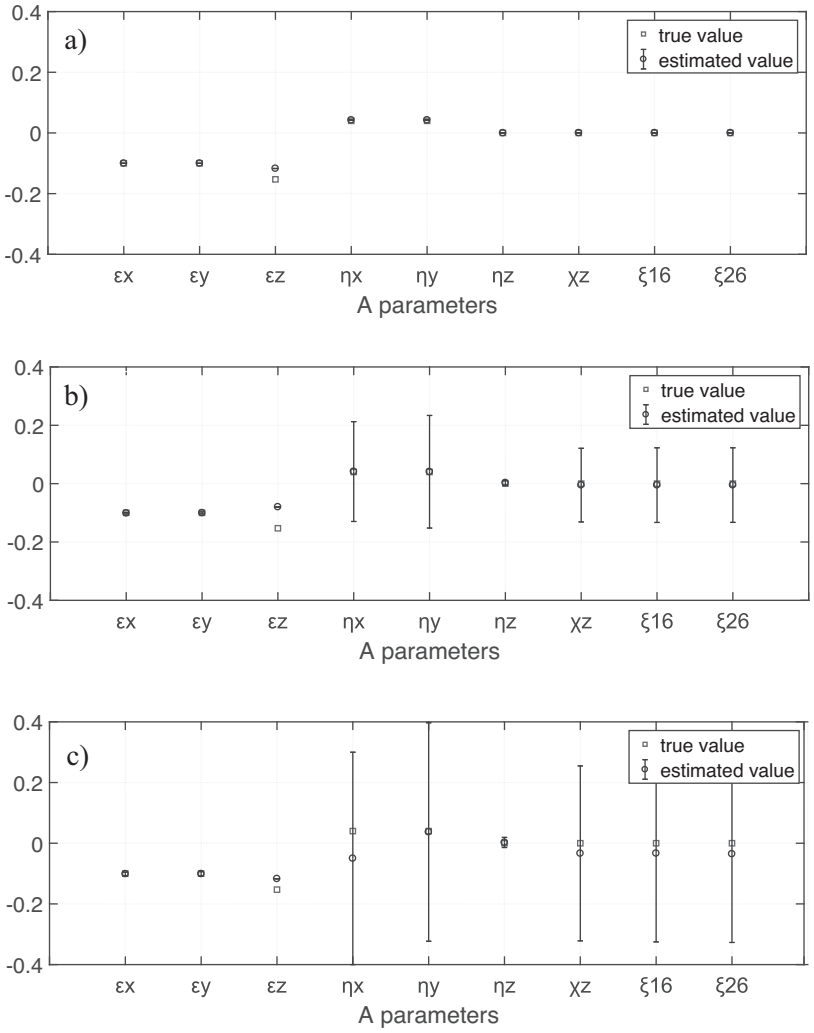

Fig. 5. Results of the inversion of traveltime data generated in the model A (VTI) with (a) no noise, (b) 2 ms and (c) 4 ms random Gaussian noise added to traveltimes generated by ANRAY package. True (squares) and estimated (circles) A-parameters. Thick vertical lines are error bars (3× exaggerated); reference velocity $\alpha = 3.6$ km/s. True thickness $H = 0.2$ km of the layer is estimated in (a) $H = 0.21$ km, in (b), $H = 0.22$ km and in (c), $H = 0.21$ km.

in Fig. 5a. The only slight difference of ε_z is caused by the difference between true value of H, $H = 0.2$, and the estimated value, $H = 0.21$. Equal values of ε_x and ε_y and of η_x and η_y, and zero value of η_z indicate that the studied medium is VTI, see Eq. (A.3) of Appendix A. Introduction of noise leads to a higher uncertainty of estimates of A-parameters η_x, η_y, ε_{16}, ε_{26} and χ_z. It increases with increasing noise. Misfit of ε_z in Fig. 5b and c is caused by the slight overestimate of H, $H = 0.22$ km in Fig. 5b and $H = 0.21$ km in Fig. 5c.

An interesting consequence of the above test is that the revelation of the model A as VTI allows an approximate reconstruction of its phase velocity. For its reconstruction, it is sufficient to know three A-parameters, ε_x, η_y and ε_z. The results of such a reconstruction are shown in Fig. 6. In Fig. 6a, the approximate phase-velocity surface calculated from true A-parameters inserted to Eq. (A.1) is shown. It is compared with phase-velocity surfaces calculated from A-parameters estimated from traveltimes with 2 ms (Fig. 6b) and 4 ms (Fig. 6c) random Gaussian noise. We can see that the main differences concentrate in polar regions controlled by A-parameters ε_z, η_x and η_y. The main difference between Fig. 6b and 6a results from the difference in ε_z, which is caused by the difference between true and estimated H. If we take into account that the overestimate of H might be about 5%, we could correct the estimated value of H closer to its true value, and thus we could obtain even better fit of plots in Fig. 6b and 6a. The eccentricity in the polar region of Fig. 6c is caused by the difference between true and estimated η_x, see Fig. 5c.

As a next model, model B, we took again the VTI layer, whose anisotropy is now stronger, approximately 15%. Thickness of the VTI layer is $H = 0.4$ km. Its matrix of density-normalized elastic moduli is shown in Eq. (C.2). A-parameters of the VTI layer, see Eq. (A.3), are $\varepsilon_x = -0.161$, $\eta_y = -0.139$, $\varepsilon_z = -0.239$. Specific feature of this model consists in its great difference of Thomsen's (1986) parameters $\varepsilon - \delta$, which makes, approximately, 0.27. Xiao et al. (2004) studied three different commonly used traveltime approximations for the estimation of Thomsen's (1986) parameters of VTI symmetry. They came to the conclusion that none of the approximations is suitable for estimating anisotropy parameters when the absolute value of $\varepsilon - \delta$ exceeds 0.2. Model B obviously belongs to this category.

Model covariance matrix is nearly identical to that shown in Fig. 4.

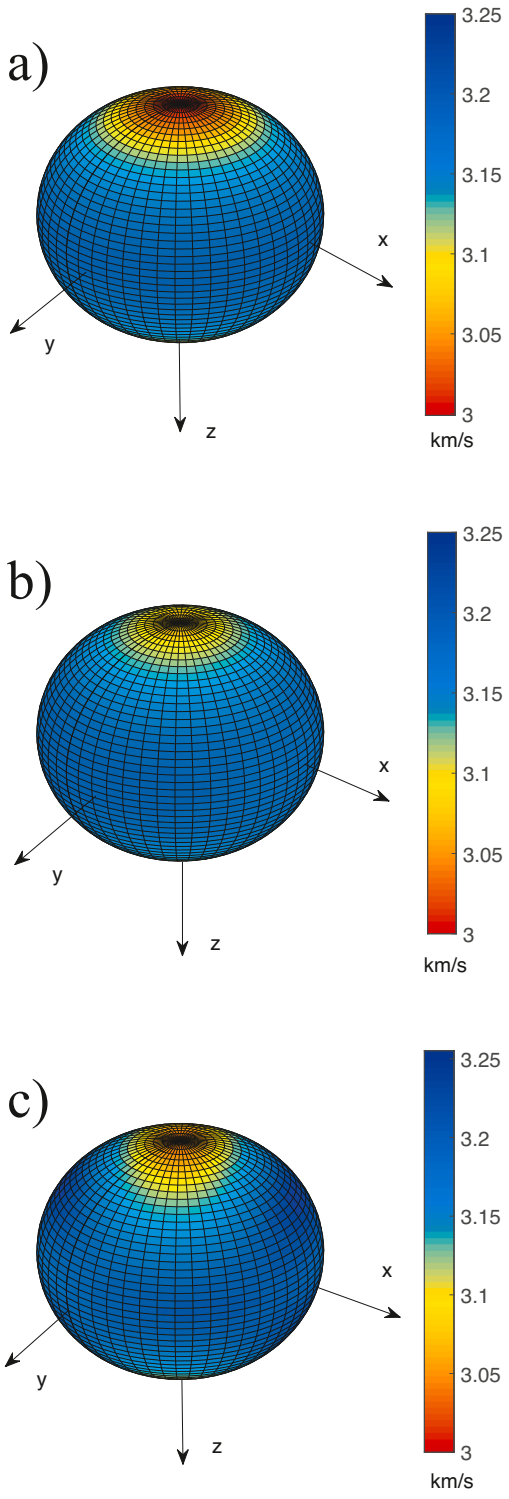

Fig. 6. First-order P-wave phase velocity surfaces for the model A (VTI) calculated from (a) true A-parameters, and A-parameters estimated from the inversion of traveltimes with (b) 2 ms and (c) 4 ms random Gaussian noise.

Results of the inversion for values of H minimizing T_{AV} in Eq. (7) are shown in Fig. 7. Again estimated A-parameters are represented by circles, true A-parameters are represented by squares. Except ε_z, A-parameters estimated from noiseless traveltimes (Fig. 7a) fit perfectly their true counterparts. The misfit of ε_z is caused by the overestimate of the thickness H. Eq. (7) provided the minimum value of T_{AV} for $H = 0.44$ km. A-parameters estimated by the inversion of traveltimes with 2 ms (Fig. 7b) and 4 ms (Fig. 7c) fit their true counterparts again quite well. Some misfit can be observed, in addition to ε_z, also on A-parameters η_x and η_z. The misfit of ε_z is caused again by the overestimate of H. In case of 2 ms noise, $H = 0.43$ km, in case of 4 ms noise, $H = 0.44$ km. As in the case of model A, it is possible to deduce from

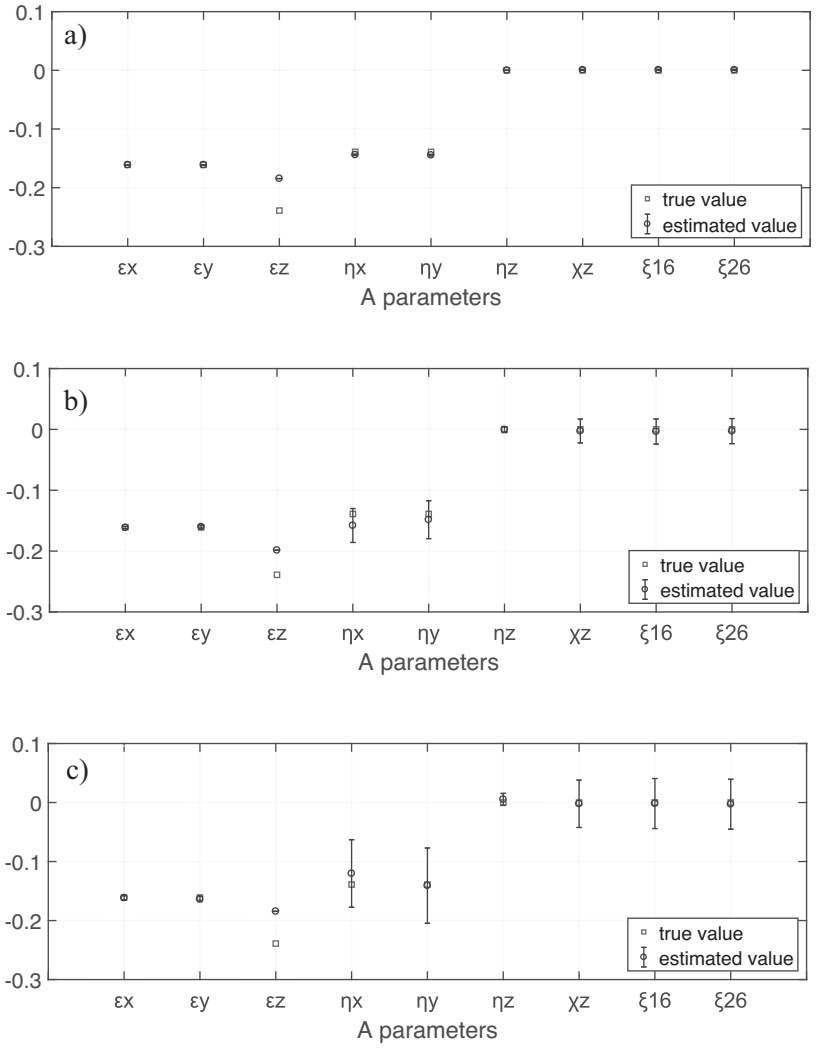

Fig. 7. Results of the inversion of traveltime data generated in the model B (VTI) with (a) no noise, (b) 2 ms and (c) 4 ms random Gaussian noise added to traveltimes generated by ANRAY package. True (squares) and estimated (circles) A-parameters. Thick vertical lines are error bars (3× exaggerated); reference velocity: $\alpha = 3.6$ km/s. True thickness $H = 0.4$ km of the layer is estimated in (a) $H = 0.44$ km; (b) $H = 0.43$ km and (c) $H = 0.44$ km.

results shown in plots in Fig. 7 that the studied layer is VTI.

The last model, model C, is a model of a layer with lowest anisotropy symmetry, the layer is triclinic. Thickness of the layer is $H = 0.7$ km. The 6×6 matrix of the density normalized elastic moduli in Voigt notation specifying model C is shown in Eq. (C.3). Corresponding A-parameters of the layer are $\varepsilon_x = 0.264$, $\varepsilon_y = 0.495$, $\varepsilon_z = 0.298$, $\eta_x = 0.015$, $\eta_y = 0.389$, $\eta_z = -0.091$, $\xi_{16} = -0.059$, $\xi_{26} = 0.083$ and $\chi_z = 0.015$.

Variation of estimated A-parameters with assumed layer thickness H for traveltimes with 4 ms random noise is shown in Fig. 8. It is interesting that although we deal with the lowest anisotropy symmetry, the only A-parameters significantly varying with H are the same as in the case of the VTI layer: ε_z, η_x and η_y. Slight variation can be also observed on A-parameter η_z. The rest of A-parameters remains constant. This means that even in the most general anisotropy, A-parameters ε_x, ε_y, ξ_{16}, ξ_{26} and χ_z can be well estimated by assuming an arbitrary reasonable value of H. In contrast to Fig. 3 showing the variation of A-parameters in the VTI layer, constant A-parameters in Fig. 8 have different values. This indicates that we are dealing either with tilted high-symmetry anisotropy or with low-symmetry anisotropy.

Model covariance matrix for model C resembles the matrix shown in Fig. 4. Because all A-parameters are non-zero, the variances are stronger and all A-parameters display weak correlation with others. Fig. 9 shows again comparison of estimated A-parameters with their true counterparts. We can observe surprisingly good fit of A-parameters ε_x, ε_y and χ_z, and even of all three η A-parameters. The misfit of A-parameters ξ_{16} and ξ_{26} is probably related to their relation to the horizontal propagation, see Eq. (A.1). Similar problems with these A-parameters were observed by Pšenčík et al. (2020). The misfit of ε_z is caused, as in previous cases, by inaccurate estimate of H. In Fig. 9a, H was estimated as $H = 0.72$ km. For the 2 ms noise in Fig. 9b, H was estimated between 0.7 and 0.75 km, for

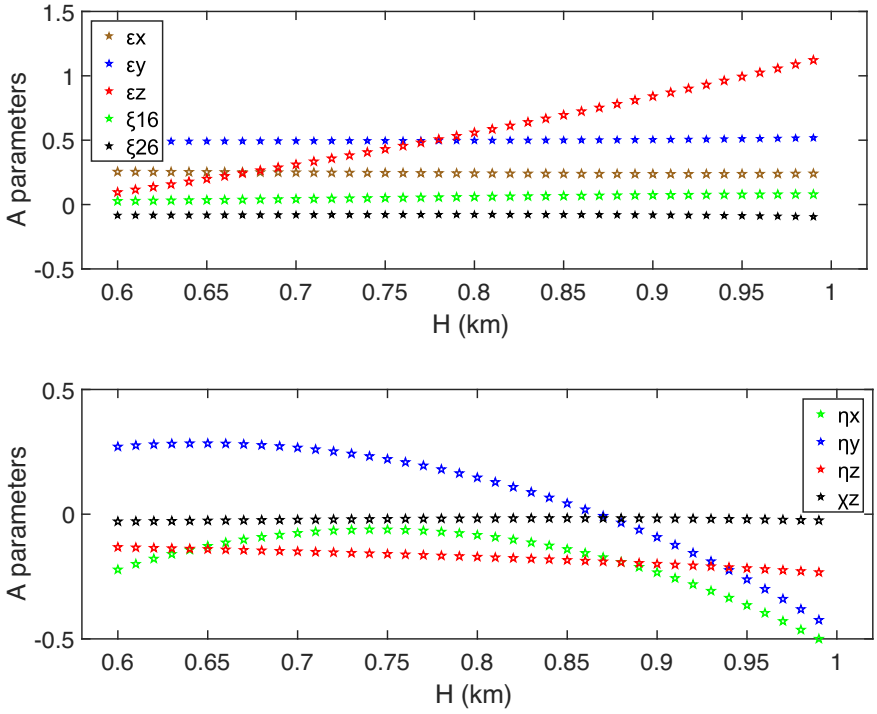

Fig. 8. Variation of estimated A-parameters with assumed thickness H in the model C (TRI). Reference velocity $\alpha = 3.6$ km/s, traveltimes with 4 ms random Gaussian noise used.

4 ms noise in Fig. 9c, between 0.65 and 0.82 km.

4. Conclusion

Weak-anisotropy approximation of P-wave moveout formula is used as a tool for the estimation of anisotropy parameters of a homogeneous layer of arbitrary anisotropy from reflection traveltimes recorded on the surface of the layer. If the thickness of the layer is unknown, it can also be estimated. A-parameters are used for the parameterization of the medium. A-parameters represent a generalization of Thomsen's parameters for anisotropy of arbitrary symmetry, orientation and strength. The use of the approximate moveout formula allows recovery of nine of fifteen A-parameters specifying, approximately, P-wave propagation in weakly anisotropic media. As expected, the accuracy of estimated A-parameters decreases with increasing anisotropy strength. Performed tests show, however, that reasonable estimates of A-parameters can be obtained even for anisotropy whose strength exceeds 20%. The tests also show that the procedure works reliably even when the difference of Thomsen's parameters $\varepsilon - \delta$ exceeds 0.2. This value represents a limit of applicability of some of commonly used P-wave moveout approximations. Successful recovery of the involved A-parameters depends on the used offsets. Numerical tests indicate that sufficiently accurate estimates of the thickness H of a layer and of its A-parameters can be obtained if normalized offsets $\overline{x}$ attain values of, at least, 3.5.

A-parameters ε_x, ε_y, ξ_{16}, ξ_{26}, χ_z, and partially also η_z can be estimated accurately even without precise knowledge of the thickness of the layer. On the contrary, A-parameters η_x, η_y and ε_z are sensitive to the accurate estimate of the thickness of the layer. Thickness can be estimated by an iterative procedure during which minimum average traveltime misfit is sought. Approximate character of the inversion formula leads to a slight overestimate of the layer thickness, which increases with the layer thickness. Performed tests indicate that the overestimate represents, at most, 5% of the layer thickness. Higher overestimates may occur only in extreme cases. Parameteres η_x and η_y are parameters with greatest variation and mutual correlation. Weaker correlation also exists among A-parameters χ_z, ξ_{16} and ξ_{26}. Generally, variations and correlations increase with increasing number of non-zero A-parameters and, for the same noise level, with decreasing thickness H of the layer.

In case of higher-symmetry anisotropy, as, for example TI or orthorhombic symmetry, additional information about orientation of symmetry elements (axes, planes) can help to estimate additional A-parameters and to reconstruct the phase velocity surface of the studied medium.

The proposed inversion procedure clearly demonstrates the advantage of the parameterization of a medium by A-parameters. The same set of A-parameters can be used for the description of any anisotropy symmetry.

The proposed procedure could be extended to multilayered media by applying the layer-striping approach. It would also be possible to replace considered horizontal reflector by dipping one. Existing moveout formulae for converted P-SV waves in transversely isotropic media based on the weak-anisotropy approximation could be used for the extension of the presented procedure to converted waves.

Declaration of Competing Interest

We have neither competing financial interests nor personal relationships that could influence the work reported in this paper.

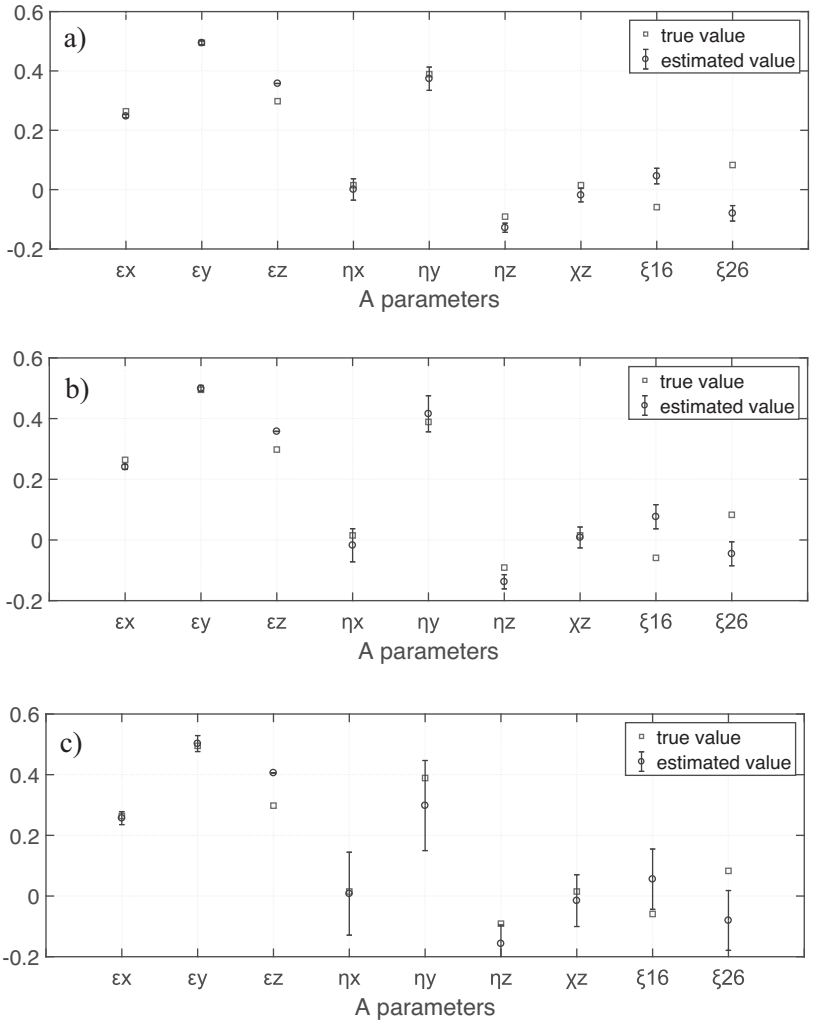

Fig. 9. Results of the inversion of traveltime data generated in the model C (TRI) with (a) no noise, (b) 2 ms and (c) 4 ms random Gaussian noise added to traveltimes generated by ANRAY package. True (squares) and estimated (circles) A-parameters. Thick vertical lines are error bars (3× exaggerated); reference velocity: $\alpha = 3.6$ km/s. True thickness $H = 0.7$ km of the layer is estimated in (a) and (b) $H = 0.72$ km, in (c) $H = 0.74$ km.

Acknowledgement

We are grateful to Qi Hao, Petr Jílek, Luděk Klimeš, Sláva Růžek, Alexey Stovas and anonymous referees for their useful comments. Han Xiao is sponsored by Chinese Scholarship Council No. 201906170237. We thank the project "Seismic waves in complex 3-D structures" (SW3D) and Research Project 20-06887S of the Grant Agency of the Czech Republic for support.

Appendix A. P-wave A-parameters

A-parameters are a generalization of Thomsen (1986) VTI parameters. In contrast to Thomsen's parameters, A-parameters can be used for the specification of anisotropy of arbitrary symmetry, strength and orientation. The complete set of 21 A-parameters (Pšenčík et al., 2018, 2020) represents an alternative to 21 independent elements of the stiffness tensor. In the weak-anisotropy approximation, it is possible to study P- and S-waves separately. Each wave mode is then specified by only 15 A-parameters. Square of the P-wave phase velocity v in the direction of a unit vector $\mathbf{N}$ specified by 15 P-wave A-parameters reads:

$$\begin{aligned} v^2(\mathrm{N}) \;=\; & \alpha^2[1 + 2(\varepsilon_x N_1^2 + \varepsilon_y N_2^2 + \varepsilon_z N_3^2 + \eta_x N_2^2 N_3^2 + \eta_y N_1^2 N_3^2 + \eta_z N_1^2 N_2^2) \\ & + 4(\chi_x N_2 N_3 + \chi_y N_1 N_3 + \chi_z N_1 N_2 - \xi_{24} N_2^3 N_3 - \xi_{34} N_2 N_3^3 - \xi_{15} N_1^3 N_3 \\ & - \xi_{35} N_1 N_3^3 - \xi_{16} N_1^3 N_2 - \xi_{26} N_1 N_2^3)]. \end{aligned} \tag{A.1}$$

A-parameters used in Eq. (A.1) are defined as follows:

$$\begin{aligned}
\varepsilon_x &= \frac{A_{11}-\alpha^2}{2\alpha^2}, \quad \varepsilon_y = \frac{A_{22}-\alpha^2}{2\alpha^2}, \quad \varepsilon_z = \frac{A_{33}-\alpha^2}{2\alpha^2}, \\
\chi_x &= \frac{A_{14}+2A_{56}}{\alpha^2}, \quad \chi_y = \frac{A_{25}+2A_{46}}{\alpha^2}, \quad \chi_z = \frac{A_{36}+2A_{45}}{\alpha^2}, \\
\eta_x &= \frac{2(A_{23}+2A_{44})-A_{22}-A_{33}}{2\alpha^2}, \quad \eta_y = \frac{2(A_{13}+2A_{55})-A_{33}-A_{11}}{2\alpha^2}, \\
\eta_z &= \frac{2(A_{12}+2A_{66})-A_{11}-A_{22}}{2\alpha^2}, \\
\xi_{24} &= \frac{A_{14}+2A_{56}-A_{24}}{\alpha^2}, \quad \xi_{34} = \frac{A_{14}+2A_{56}-A_{34}}{\alpha^2}, \quad \xi_{15} = \frac{A_{25}+2A_{46}-A_{15}}{\alpha^2}, \\
\xi_{35} &= \frac{A_{25}+2A_{46}-A_{35}}{\alpha^2}, \quad \xi_{16} = \frac{A_{36}+2A_{45}-A_{16}}{\alpha^2}, \quad \xi_{26} = \frac{A_{36}+2A_{45}-A_{26}}{\alpha^2}.
\end{aligned} \tag{A.2}$$

The symbol α used in Eqs. (A.1) and (A.2) is a reference P-wave velocity in a reference isotropic medium. The symbols $A_{\alpha\beta}$ denote the elements of the 6×6 matrix of the density-normalized elastic parameters in the Voigt notation.

The moveout Eq. (1) with (2) depends on only nine of the above fifteen A-parameters, specifically on ε_x, ε_y, ε_z, η_x, η_y, η_z, χ_z, ξ_{16} and ξ_{26}. In VTI symmetry, the number of independent A-parameters farther reduces because some of the A-parameters satisfy the conditions:

$$\varepsilon_x = \varepsilon_y, \quad \eta_x = \eta_y, \quad \eta_z = \chi_z = \xi_{16} = \xi_{26} = 0. \tag{A.3}$$

In isotropic media, the additional conditions apply:

$$\varepsilon_x = \varepsilon_y = \varepsilon_z, \quad \eta_x = \eta_y = \eta_z = \chi_z = \xi_{16} = \xi_{26} = 0. \tag{A.4}$$

Appendix B. Inversion procedure

We start with Eq. (8):

$$\mathrm{Gm} = \mathrm{d}. \tag{B.1}$$

The symbol **G** represents the $N \times M$ matrix, where N is the number of observations and M is the number of sought A-parameters. In our case $M = 8$. The rows of matrix **G** have the following form:

$$\begin{aligned}
&\left(\bar{x}^2(1+\bar{x}^2)cos^2\phi, \quad \bar{x}^2(1+\bar{x}^2)sin^2\phi, \quad \bar{x}^2sin^2\phi, \quad \bar{x}^2cos^2\phi, \quad \bar{x}^4cos^2\phi sin^2\phi,\right. \\
&\left. 2\bar{x}^2(1+\bar{x}^2)cos\phi sin\phi, \quad -2\bar{x}^4cos^3\phi sin\phi, \quad -2\bar{x}^4cos\phi sin^3\phi\right).
\end{aligned} \tag{B.2}$$

Each row in matrix **G** corresponds to one particular receiver.

Symbol **m** in Eq. (B.1) is the eight-dimensional vector of model parameters to be determined. It consists of eight P-wave A parameters m_i ordered as:

$$\mathrm{m} \equiv (\varepsilon_x, \ \varepsilon_y, \ \eta_x, \ \eta_y, \ \eta_z, \ \chi_z, \ \xi_{16}, \ \xi_{26})^T. \tag{B.3}$$

The symbol T indicates transposition.

Vector **d** in Eq. (B.1) has the following form:

$$\begin{aligned}
\mathrm{d} \equiv \frac{1}{2}\Bigg(&\left(1+\bar{x}_1^2\right)\left[\left(\frac{T_0^2(1+\bar{x}_1^2)}{T_{\mathrm{obs}}^2(x_1,\phi_1)}-1\right)(1+\bar{x}_1^2)-\frac{T_0^2-T_{\mathrm{obs}}^2(0)}{T_{\mathrm{obs}}^2(0)}\right] \\
&\left(1+\bar{x}_2^2\right)\left[\left(\frac{T_0^2(1+\bar{x}_2^2)}{T_{\mathrm{obs}}^2(x_2,\phi_2)}-1\right)(1+\bar{x}_2^2)-\frac{T_0^2-T_{\mathrm{obs}}^2(0)}{T_{\mathrm{obs}}^2(0)}\right], \quad \ldots \\
&\left(1+\bar{x}_N^2\right)\left[\left(\frac{T_0^2(1+\bar{x}_N^2)}{T_{\mathrm{obs}}^2(x_N,\phi_N)}-1\right)(1+\bar{x}_N^2)-\frac{T_0^2-T_{\mathrm{obs}}^2(0)}{T_{\mathrm{obs}}^2(0)}\right]\Bigg)^T.
\end{aligned} \tag{B.4}$$

Eq. (B.1) represents an overdetermined system of linear equations. It can be solved by pseudoinverse (e.g., Press et al., 2007; Aster et al., 2013):

$$\mathrm{m} = \mathrm{G}^\dagger \mathrm{d}, \tag{B.5}$$

where $\mathbf{G}^\dagger$ denotes the pseudoinverse of matrix **G**.

An important part of the inversion is the assessment of errors of estimated A-parameters. We follow Pšenčík et al. (2020) and transform the data covariance matrix $\mathbf{C}_d$ to the model covariance matrix $\mathbf{C}_m$:

$$\mathrm{C}_m = \mathrm{G}^\dagger \mathrm{C}_d \mathrm{G}^{\dagger T}. \tag{B.6}$$

Instead of the unknown exact data covariance matrix $\mathbf{C}_d$, we use its approximation:

$$\mathbf{C}_d \approx \sigma^2 \mathbf{I}, \tag{B.7}$$

where **I** is the 8×8 identity matrix. The value of the parameter σ is determined using χ^2 statistics of residuals $\mathbf{r} = \mathbf{d} - \mathbf{Gm}$ with the number of degree of freedom $\nu = N - M$. We get

$$\sigma = \sqrt{\nu^{-1}\mathrm{r}^T\mathrm{r}}, \tag{B.8}$$

see Eq. (A-10) of Pšenčík et al. (2020).

Using Eq. (B.6), we can estimate the model covariance matrix $\mathbf{C}_m$. Square roots of diagonal elements of $\mathbf{C}_m$ then represent Gaussian errors of individual A-parameters expressed as error bars in the plots of A-parameters estimates. Note that the Gaussian error of the A-parameter ε_z is zero because ε_z is calculated exactly from Eq. (5).

Appendix C. Matrices of the density-normalized elastic moduli of the tested models

Model A consists of the layer of transversely isotropic limestone with the vertical axis of symmetry (VTI). The matrix of the density-normalized elastic moduli in $(km/s)^2$ reads:

$$\begin{pmatrix} 10.368 & 4.540 & 4.369 & 0 & 0 & 0 \\ & 10.368 & 4.369 & 0 & 0 & 0 \\ & & 9.000 & 0 & 0 & 0 \\ & & & 2.914 & 0 & 0 \\ & & & & 2.914 & 0 \\ & & & & & 2.914 \end{pmatrix} \tag{C.1}$$

Anisotropy strength of model A is about 8%.

Model B is also VTI. Its matrix of the density-normalized elastic moduli in $(km/s)^2$ reads:

$$\begin{pmatrix} 8.788 & -1.612 & -2.029 & 0 & 0 & 0 \\ & 8.788 & -2.029 & 0 & 0 & 0 \\ & & 6.760 & 0 & 0 & 0 \\ & & & 4.000 & 0 & 0 \\ & & & & 4.000 & 0 \\ & & & & & 5.200 \end{pmatrix} \tag{C.2}$$

Anisotropy strength of the model is about 15%. The model is specific by a great difference $\varepsilon - \delta \sim 0.27$. Here ε and δ are Thomsen's (1986) parameters.

Model C consists of the layer of triclinic symmetry (Grechka, 2020). The matrix of the density-normalized elastic moduli in $(km/s)^2$ reads:

$$\begin{pmatrix} 19.810 & 8.620 & 9.000 & -2.370 & -1.440 & 0.950 \\ & 25.790 & 9.090 & 0.570 & -0.990 & -0.890 \\ & & 20.680 & -2.100 & 0.430 & 0.490 \\ & & & 7.170 & -0.150 & -0.0800 \\ & & & & 8.140 & -0.330 \\ & & & & & 6.490 \end{pmatrix} \tag{C.3}$$

Anisotropy strength is approximately 17%.

References

Aster, R.C., Borchers, B., Thurber, C.H., 2013. Parameter Estimation and Inverse Problems. Academic Press, Oxford.

Farra, V., Pšenčík, I., 2016. Weak-anisotropy approximations of *P*-wave phase and ray velocities for anisotropy of arbitrary symmetry. Stud. Geophys. Geod. 60, 403–418.

Farra, V., Pšenčík, I., 2021. Weak-anisotropy approximation of *P*-wave geometrical spreading in horizontally layered anisotropic media of arbitrary symmetry. TTI specification. Geophysics 86, C119–C132.

Farra, V., Pšenčík, I., Jílek, P., 2016. Weak-anisotropy moveout approximations for *P*-waves in homogeneous layers of monoclinic or higher anisotropy symmetries. Geophysics 81, C39–C59.

Fomel, S., Stovas, A., 2010. Generalized nonhyperbolic moveout approximation. Geophysics 75, U9–U18.

Gajewski, D., Pšenčík, I., 1990. Vertical seismic profile synthetics by dynamic ray tracing in laterally varying layered anisotropic structures. J. Geophys. Res. 95, 11301–11315.

Grechka, V., 2020. Moment tensors of double-couple microseismic sources in anisotropic formations. Geophysics 85, 1JF-Z3.

Grechka, V., Pech, A., Tsvankin, I., 2005. Parameter estimation in orthorhombic media using multicomponent wide-azimuth reflection data. Geophysics 70, D1–D8.

Press, W.H., Flannery, B.P., Teukolsky, S.A., Vetterling, W.T., 2007. Numerical Recipes. Cambridge University Press, Cambridge.

Pšenčík, I., Farra, V., 2017. Reflection moveout approximations for *P*-waves in a moderately anisotropic homogeneous tilted transverse isotropy layer. Geophysics 82, C175–C185.

Pšenčík, I., Gajewski, D., 1998. Polarization, phase velocity and NMO velocity of *qP*-waves in arbitrary weakly anisotropic media. Geophysics 63, 1754–1766.

Pšenčík, I., Růžek, B., Lokajíček, T., Svitek, T., 2018. Determination of rock-sample anisotropy from *P* and *S*-wave traveltime inversion. Geophys. J. Int. 214, 1088–1104.

Pšenčík, I., Růžek, B., Jílek, P., 2020. Practical concept of traveltime inversion of simulated *P*-wave vertical seismic profile data in weak to moderate arbitrary anisotropy. Geophysics 85, C107–C123.

Sripanich, Y., Fomel, S., Stovas, A., Hao, Q., 2017. 3D generalized nonhyperboloidal moveout approximation. Geophysics 82, C49–C59.

Thomsen, L., 1986. Weak elastic anisotropy. Geophysics 51, 1954–1966.

Tsvankin, I., Grechka, V., 2011. Seismology of Azimuthally Anisotropic Media and Seismic Fracture Characterization. SEG.

Tsvankin, I., Thomsen, L., 1994. Nonhyperbolic reflection moveout in anisotropic media. Geophysics 59, 1290–1304.

Xiao, C., Bancroft, J.C., Brown, R.J., 2004. Estimation of anisotropy parameters in VTI media. SEG Expand. Abstr. 23, 119. https://doi.org/10.1190/1.1851093.

Xiao, H., Pšenčík, I., 2020. Determination of *P*-wave anisotropic parameters and thickness of a single layer of arbitrary anisotropy from traveltimes of a reflected *P*-wave. In: Seismic Waves in Complex 3-D Structures, vol. 30, pp. 9–28. http://sw3d.cz.